Observational Study

Medicine®

OPEN

Predictive model for the diagnosis of benign/malignant small pulmonary nodules

Weisong Chen, MS[a], Dan Zhu, MS[a], Hui Chen, MS[a], Jianfeng Luo, MS[a], Haiwei Fu, MS[b,*]

Abstract

There is some doubt that all nodules <8 mm are really mainly benign and that simple follow-up is adequate in all cases. The purpose of this study is to create a predictive model for the diagnosis of benign and malignant small pulmonary nodules.

This was a retrospective case–control study of patients who had undergone pulmonary nodule resection at the Zhejiang University Jinhua Hospital. Patients with pulmonary nodules of ≤10 mm in size on chest high-resolution computed tomography were included. Patients' demographic characteristics, clinical features, and high-resolution computed tomography findings were collected. Logistic regression and receiver-operating characteristic analysis were used to create a predictive model for malignancy.

A total of 216 patients were included: 160 with malignant and 56 with benign nodules. Nodule density (odds ratio [OR] = 0.996, 95% confidence interval [CI]: 0.993–0.998, $P = .001$), vascular penetration sign (OR = 3.49, 95% CI: 1.39–8.76, $P = .008$), nodule type (OR = 4.27, 95% CI: 1.48–12.29, $P = .007$), and incisure surrounding nodules (OR = 0.18, 95% CI: 0.04–0.84, $P = .03$) were independently associated with malignant nodules. These factors were used to create a mathematical model that had an area under the receiver-operating characteristic curve of 0.744. Using a cut-off of 0.762 resulted in 63.1% sensitivity and 75.0% specificity.

This study proposes a pulmonary nodule prediction model that can estimate benign/malignant lung nodules with good sensitivity and specificity. Mixed ground-glass nodules, vascular penetration sign, density of lung nodules, and the absence of incisure signs are independently associated with malignant lung nodules.

Abbreviations: CI = confidence interval, CT = computed tomography, HRCT = high-resolution computed tomography, mGNN = mixed ground-glass nodules, pGNN = pure ground-glass nodules, SD = standard deviation.

Keywords: benign, computed tomography, malignant, predictive value of tests, pulmonary nodule

1. Introduction

Lung cancer causes an estimated 1.6 million deaths every year, being the leading cause of cancer-related deaths in the world.[1–3] In China, lung cancer is the most common cancer and ranks 1st among the causes of cancer-related deaths, at 24.4%.[4,5] Tobacco use, occupational exposure (such as asbestos, coal, or silica), and family history of lung cancer are the 3 main risk factors.[6–8] Although smoking is the main risk factor for lung adenocarcinoma, it is not the only one, and nonsmokers can develop lung cancer, but lung cancer in never-smokers is a heterogeneous group of diseases.[9] In China, the rates of tobacco use and environmental exposure are high, especially in the setting where many households still use coal for heating and cooking.[10,11]

As for any cancer, early diagnosis of lung cancer yields the best prognosis, with a 5-year survival of 82% for stage IA and 6% for stage IV.[12] Unfortunately, many early stage lung cancers are asymptomatic and are at an advanced stage when discovered.[13] If lung cancer could be clinically diagnosed early, the prognosis of patients could be significantly improved.

Chest computed tomography (CT) is a commonly used imaging examination. The detection rate of lung nodules is much higher with CT than with an X-ray examination, and the National Lung Screening Trial showed that LDCT could reduce lung cancer mortality by 20%.[14,15] Indeed, the detection rates for stages I, II, III, and IV lung cancer were 50%, 7%, 21%, and 22%, respectively, in the low dose spiral computed tomography (LDCT) arm, compared to 31%, 8%, 25%, and 36% in the chest X-ray arm. Therefore, LDCT is currently the best screening method for lung cancer, but the qualitative diagnosis of pulmonary nodules remains a difficult problem for clinicians. Indeed, the nature of pulmonary nodules is confirmed by invasive or minimally invasive pathologic examination, with significant burdens to the patient and the healthcare system.

Nomograms are attempting to predict the likelihood of malignancy of lung nodules. A prospective study showed that the malignancy rate of nodules of <5 mm was 0.4%, while the rates were 1.3% for nodules of 5 to 10 mm and 15.3% for nodules >10 mm.[16] According to the pulmonary nodule guidelines, pulmonary nodules of >8 mm are generally of concern by clinicians, while nodules <8 mm are also of concern, but the clinicians are often limited in what they can offer other than serial follow-up.[17]

Editor: Danny Chu.

The authors have no funding and conflicts of interest to disclose.

[a] Jinhua Hospital of Zhejiang University, Jinhua Central Hospital, Jinhua, [b] Taizhou First People's Hospital, Taizhou, Zhejiang, China.

[*] Correspondence: Haiwei Fu, Taizhou First People's Hospital, Taizhou, Zhejiang, China (e-mail: fuhaiwei9280@163.com).

How to cite this article: Chen W, Zhu D, Chen H, Luo J, Fu H. Predictive model for the diagnosis of benign/malignant small pulmonary nodules. Medicine 2020;99:15(e19452).

Received: 26 June 2019 / Received in final form: 11 November 2019 / Accepted: 7 February 2020

http://dx.doi.org/10.1097/MD.0000000000019452

Nevertheless, there is some doubt that all nodules <8 mm are really mainly benign and that simple follow-up is adequate in all cases. Therefore, the aim of the present study was to collect and analyze the data of pulmonary nodules that were pathologically diagnosed at our hospital. The results should provide a better understanding of the judgment of benign vs malignant pulmonary nodules, and subsequently improve the rate of early lung cancer diagnosis.

2. Materials and methods

2.1. Study design and patients

This was a retrospective case–control study of patients who had undergone pulmonary nodule resection at the Zhejiang University Jinhua Hospital between January 2015 and March 2018. The inclusion criterion was patients with pulmonary nodules of ≤10 mm in size on preoperative chest high-resolution CT (HRCT). The exclusion criteria were: 10% increase in maximum diameter within 3 months; personal or family history of tumor; or lesions completely calcified.

The study was approved by the ethics committee of Zhejiang University Jinhua Hospital and was conducted in accordance with the Helsinki Declaration of 1964 (revised 2008). The need for individual consent was waived by the committee.

2.2. Evaluation of CT features

The HRCT was conducted with a 64-detector CT scanner (Philips iCT 256 or Philips Brilliance 64, The Netherlands). Targeted thin-section helical CT scans were obtained from the lung apices to the level of the middle pole of both kidneys. Three-dimensional reconstruction methods were performed with a CT layer thickness of 1 mm. Two chest radiologists with at least 5 years of working experience independently read each chest CT examination. The radiologists were blind to the pathology results. Any inconsistencies were resolved by discussion to reach a consensus.

If the patient had multiple nodules, only the nodule with the largest diameter was included in this study. Pulmonary nodules were classified as being on the left or right side, as being in the upper, middle, or lower lobe (the lingual lobe was classified as the middle lobe), and as being single or multiple. The long and short axes of the nodules were measured, and the ratio of the short to long axis was calculated. Radiologic signs such as spiculation (sunburst appearance), cavitation sign (gas-filled space seen as a lucency or low-attenuation area), calcification, vascular penetration sign (when a pulmonary artery passes through the nodule), pleural adhesions, incisure surrounding nodules (a notch in the outer wall), nodules average density, and nodular type (solid, mixed, and pure ground glass) were described.[18–20] The nodules were classified into solid nodules (appearing as solid nonhazy nodules), mixed ground-glass nodules (mGGN, appearing as nodules with both hazy and nonhazy areas), and pure ground-glass nodules (pGGN, appearing as an area of hazy increased attenuation).[18]

2.3. Data collection

Sex, age, smoking history, personal tumor history, and family history of cancer were collected. Smoking was defined as smoking for >6 months, including being exposed to secondhand smoke. The cases in this study were from 2015 to 2018; therefore, some cases were pathologically diagnosed according to the old histologic classification (2004 WHO classification of tumors of the lung, pleura, thymus, and heart). The specimens were reclassified according to the 2015 WHO classification of tumors of the lung, pleura, thymus, and heart).[19]

2.4. Statistical analysis

The SPSS 19.0 (IBM Corp, Armonk, NY) was used for statistical analysis. Categorical variables are presented as frequencies and percentages and were analyzed using the Chi-squared test or Fisher exact test, as appropriate. Continuous variables were tested for normality using the Kolmogorov–Smirnov test. Normally distributed continuous variables are presented as mean ± standard deviation and were compared using the Student *t* test. Non-normally distributed continuous variables are presented as median (range) and were compared using the Mann–Whitney *U* test. Multivariable logistic regression analysis was used to identify the factors independently associated with malignant pulmonary nodules. A prediction model was established for the risk of a pulmonary nodule of being malignant. Receiver-operating characteristic analysis was conducted for the prediction model. $P < .05$ was considered statistically significant.

3. Results

3.1. Characteristics of the patients

A total of 216 patients met the inclusion criteria, including 160 cases of malignant nodules and 56 cases of benign nodules. Among all patients, there were 21 smokers and 195 nonsmokers, and the patients were 51.2 ± 10.9 years. There were no differences between the 2 groups regarding age, gender, location, and number of nodules (all $P > .05$), but there was a lower frequency of smokers in the malignant nodule group (5.6% vs 16.1%, $P = .02$) (Table 1).

3.2. Imaging features

There were no differences between benign and malignant nodules regarding spiculation, cavitation sign, calcification, and pleural adhesions (all $P > .05$). Compared with the benign nodules, the malignant nodules showed higher frequencies of the vascular penetration sign (46.3% vs 21.4%, $P = .001$) and mGGN and pGGN (36.9% vs 16.1% and 45.6% vs 39.3%, $P < .001$), lower frequency of the incisure sign (4.5% vs 16.1%, $P = .001$), longer long axis (6.9 ± 1.7 vs 6.1 ± 2.2 mm, $P = .01$), longer short axis (5.6 ± 1.5 vs 4.8 ± 1.63 mm, $P = .002$), and higher nodule density (−632.1 ± 113.4 vs −552.0 ± 206.4 HU, $P = .007$) (Table 1). Figures 1–3 present typical cases.

3.3. Pathologic characteristics

The malignant nodule group included 2 cases of atypical adenomatous carcinoma, 87 cases of adenocarcinoma in situ, 58 cases of minimally invasive carcinoma, and 12 cases of invasive adenocarcinoma and 1 case of carcinoid. The pathologic lesion size was higher in the malignant group (6.9 ± 1.7 vs 6.1 ± 2.2 mm, $P = .01$).

3.4. Multivariable logistic regression analysis and model establishment

All the influencing factors were included in the multivariable logistic regression analysis. The results showed that only 4 factors

Table 1

Characteristics of the patients and morphologic features on high-resolution computed tomography of benign and malignant lesions.

	Benign	Malignant	*P*
N	56	160	
Age, yrs (mean ± SD)	52.9 ± 10.6	50.6 ± 11.0	.172
Gender, n (%)			.079
Male	20 (35.7%)	37 (23.1%)	
Female	36 (64.3%)	123 (76.9%)	
Smoking, n (%)	9 (16.1%)	9 (5.6%)	.023
Location, n (%)			
Left	21 (37.5%)	58 (36.3%)	.867
Right	35 (62.5%)	102 (63.8%)	
Upper	32 (57.1)	101 (63.1%)	.238
Middle	9 (16.1%)	13 (8.1%)	
Lower	15 (26.8%)	46 (28.8%)	
Number of nodules, n (%)			.055
Single	13 (23.2%)	20 (12.5%)	
Multiple	43 (76.8%)	140 (87.5%)	
Spiculation, n (%)	7 (12.5%)	20 (12.5%)	1.000
Cavitation sign, n (%)	7 (12.5%)	31 (19.4%)	0.245
Calcification, n (%)	1 (1.8%)	0	0.259
Vascular penetration sign, n (%)	12 (21.4%)	74 (46.3%)	0.001
Pleural adhesions, n (%)	12 (21.4%)	27 (16.9%)	0.446
Incisure surrounding nodules, n (%)	9 (16.1%)	4 (2.5%)	0.001
Nodule type, n (%)			<0.001
Solid	25 (44.6%)	28 (17.5%)	
Mixed	9 (16.1%)	59 (36.9%)	
Pure ground glass	22 (39.3%)	73 (45.6%)	
Long axis, mm (mean ± SD)	6.1 ± 2.2	6.9 ± 1.7	0.012
Short axis, mm (mean ± SD)	4.8 ± 1.6	5.6 ± 1.5	0.002
Ratio of short-axis to long-axis of the nodule (mean ± SD)	0.82 ± 0.14	0.82 ± 0.13	0.937
Nodule density, HU (mean ± SD)	−552.0 ± 206.4	−632.1 ± 113.4	0.007
Histology, n (%)			
Benign	56 (100%)		
Atypical adenomatous hyperplasia		2 (1.2%)	
Adenocarcinoma in situ		87 (54.4%)	
Minimally invasive carcinoma	–	58 (36.3%)	
Invasive adenocarcinoma	–	12 (7.5%)	
Carcinoid		1 (0.6%)	
Pathologic size, mm (mean ± SD)	6.1 ± 2.2	6.9 ± 1.7	0.012

SD = standard deviation.

had statistical significance: nodule density (odds ratio [OR] = 0.995, 95% confidence interval [CI]: 0.993–0.998, $P = .001$), vascular penetration sign (OR = 3.49, 95% CI: 1.39–8.76, $P = .008$), nodule type (OR = 4.27, 95% CI: 1.48–12.29, $P = .007$), and incisure surrounding nodules (OR = 0.18, 95% CI: 0.04–0.84, $P = .03$) (Table 2). Hence, the prediction equation $P = e^Z/(1 + e^Z)$ was obtained, where $z = -2.957 - (0.004*X1) + (1.096*X2) + (1.198*X3) - (1.811*X4)$, X1 was "lung nodule density" (in HU), X2 was "vascular penetration sign" (with = 1, without = 0), X3 was nodule type (mGGN = 1, solid or pGGN = 0), and X4 was incisure (with = 1, without = 0).

The omnibus testing of model coefficients (interconnected $X2 = 70.667$, df = 19, $P < .002$) indicated that the model passed the omnibus tests. The maximum likelihood ratio test showed that the maximum likelihood value (−2log likelihood) was 176.559, the Cox–Snell fitting value R2 was 0.279, and the Nagel–Kerke fitting value R2 was 0.409, indicating that the model fitting effect was good. The model passed the Hosmer–Lemeshow test ($X^2 = 4.051$, $P = .852$).

The receiver-operating characteristic curve showed that the area under the curve was 0.744 (95% CI: 0.681–0.801) (Fig. 4). By calculation, we selected 0.762 as the cutoff, which resulted in 63.1% sensitivity and 75.0% specificity.

4. Discussion

Currently, the most common cause of cancer-related death is lung cancer.[1–3] The incidence and mortality of lung cancer in China is the highest among all malignant tumors.[4,5] Most lung cancers are found at an advanced stage and have a poor prognosis. How to improve the detection rate of early lung cancer and then provide correct and reasonable treatment are the keys to improve the survival rate of lung cancer.[21] There is some doubt that all nodules <8 mm are really mainly benign and that simple follow-up is adequate in all cases. Therefore, this study aimed to collect and analyze the data of pulmonary nodules that were pathologically diagnosed at our hospital. This study proposes a pulmonary nodule prediction model that can estimate benign/malignant lung nodules with good sensitivity and specificity. Mixed ground-glass nodules, vascular penetration sign, density of lung nodules, and the absence of incisure signs are independently associated with malignant lung nodules.

In recent years, the widespread application of CT led to high numbers of pulmonary nodules being found. Guidelines indicate that pulmonary nodules <8 mm can be followed, while those >8 mm should be investigated.[17] Nevertheless, as shown in the present study, many pulmonary nodules <10 mm can be malignant. The National Lung Screening Trial found that the rate of pulmonary nodule positivity was 25%.[14] Furthermore, in the present study, the frequency of smokers in patients with malignant pulmonary nodules <10 mm was lower than in those with benign nodules, suggesting that the disease history is different from the classical lung cancer. A previous study showed that most of the lung cancers in nonsmokers were slow-growing adenocarcinomas,[22] supporting the present study. Although no causality conclusions can be drawn from a retrospective case–control study, the concept of smoking being the main risk factor for lung cancer could be revisited as smoking being the main risk factor for rapidly growing lung cancers, but this is only a hypothesis and will need additional studies. Smoking is associated with lung squamous cell carcinoma and small cell carcinoma, but the association between smoking and lung adenocarcinoma is weaker.[23] In the present study, only adenocarcinoma and carcinoid were observed, which is consistent with the low frequency of smokers. In addition, female nonsmokers are significantly more frequently affected than male nonsmokers.[9,24,25] This suggests that lung cancer can be caused in some patients by carcinogens other than those found in tobacco smoke, as previously suggested.[9] This could be particularly true in countries where air pollution, and especially particulate pollution, is very high, such as in China.[26,27] Of note, a considerable proportion of Chinese households still use coal for heating and cooking, and it has an impact on the incidence of lung cancer.[28] Those associations with pulmonary nodules <10 mm and lung cancer in nonsmokers require further study.

It was found that gender, smoking, vascular penetration sign, incisure surrounding nodules, the long axis of pulmonary nodules, short axis of pulmonary nodules, nodules average density, and nodular type were significantly associated with malignancy in the univariable analyses. The multivariable analysis showed that the density of pulmonary nodules, vascular

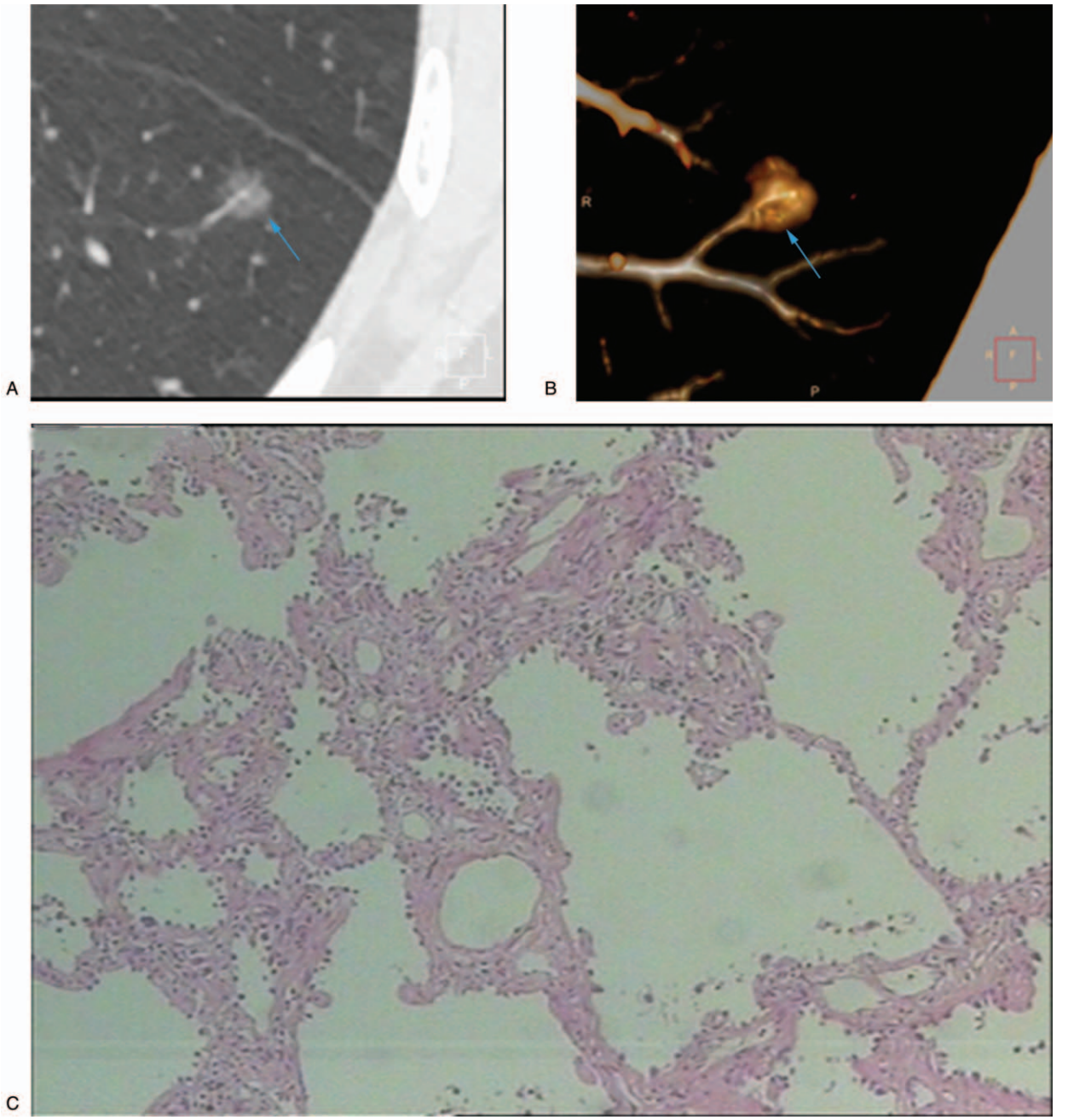

Figure 1. A 42-year-old nonsmoking woman with a peripheral pure ground-glass nodule in the left lower lobe. (A) High-resolution computed tomography showed a 7-mm nodule with the vascular penetration sign (blue arrow). (B) Three-dimensional reconstruction image of the same nodule (blue arrow). (C) The pathologic diagnosis of the resected specimen showed adenocarcinoma in situ.

penetration sign, mGGN, and incisure surrounding nodules were independently associated with malignancy.

Indeed, nodule density has been consistently associated with the probability of malignancy.[29,30] A penetrating pulmonary artery into a nodule could indicate a higher blood supply, which is needed by malignant tumors.[20] Regarding mGGN, some controversies upon their management still exist.[31,32] The present study suggests that mGGN is independently associated malignancy of pulmonary nodules <10 mm, but the results should be considered within the model established here and not as a single factor. Finally, the presence of notches in the nodule margin is considered to be associated with malignancy.[33]

Other models for predicting the malignancy of pulmonary nodules are available. The Mayo clinic lung cancer prediction model is widely used to evaluate the probability of malignant pulmonary nodule.[34] This model is based on age, smoking history, diameter, spiculation, and vascular penetration sign, but is validated for nodules >10 mm in diameter, which limits is relevancy in the context of HRCT screening. Other models include the VA model, the PKUPH model, and the Brock University model.[34,35] The present study proposes a pulmonary nodule prediction model that can estimate benign/malignant lung nodules with good sensitivity and specificity. Mixed ground-glass nodules, vascular penetration sign, density of lung nodules, and

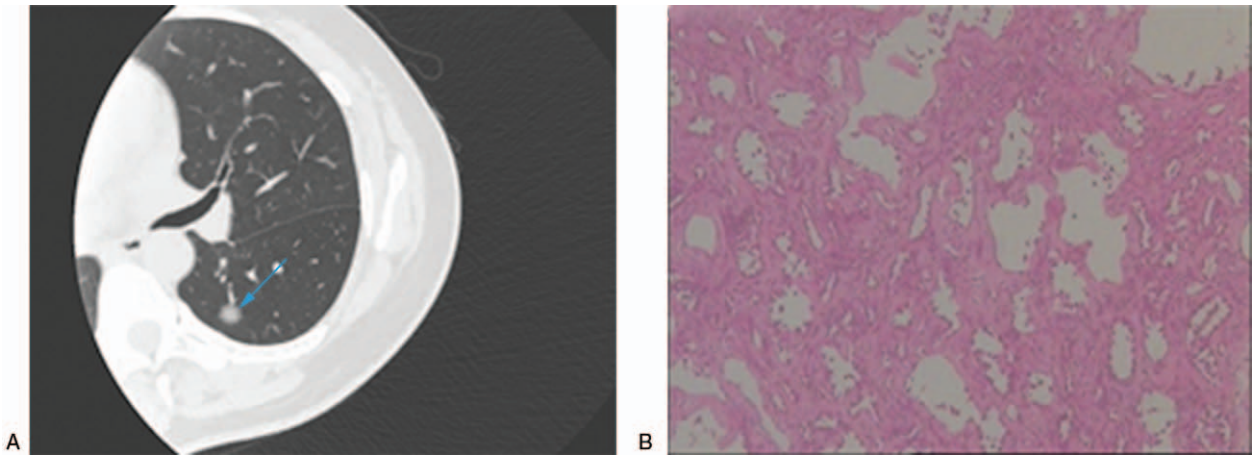

Figure 2. A 37-year-old nonsmoking woman with a peripheral mixed ground-glass nodule in the left lower lobe. (A) High-resolution computed tomography showed an 8-mm nodule (blue arrow). (B) The pathologic diagnosis of the resected specimen was minimally invasive adenocarcinoma.

the absence of incisure signs are independently associated with malignant lung nodules. Nevertheless, we agree that how this model does differ from existing models and whether it has a better predictive value remains to be determined. Future studies should compare those models using the same sample of patients to determine their relative diagnostic value.

The present study suggests that nodule location was not predictive for lung cancer, which is different from the literature. Indeed, lung cancer occurs more frequently in the upper lobes, with a predilection for the right lung.[36,37] Nevertheless, one study indicated that symptom history, family history, and upper lobe location were not associated with a risk of malignant single pulmonary nodules.[38] In the PanCan trial, a multiplicity of nodules was associated with a reduced risk of cancer compared with the risk associated with a solitary nodule.[39] In the present study, there was no statistically significant difference between single and multiple pulmonary nodules in predicting lung cancer.

There are some limitations to this study. The sample size was small, and many independent variables were evaluated. In addition, the patients were only those who had pathologic results after surgery, introducing a clear selection bias. Among the patients with lung cancer, only lung adenocarcinoma and carcinoid were observed. Since the histologic subtype was not a selection criterion, the small sample size probably precluded the observation of other cancer subtypes. Some factors were measured manually (nodule size), which inevitably will lead to some error. This was a retrospective study, limited to the data available in the charts and limiting the comparison with other predictive models. In addition, causality conclusions cannot be drawn from case–control studies. Additional studies are necessary to address these issues.

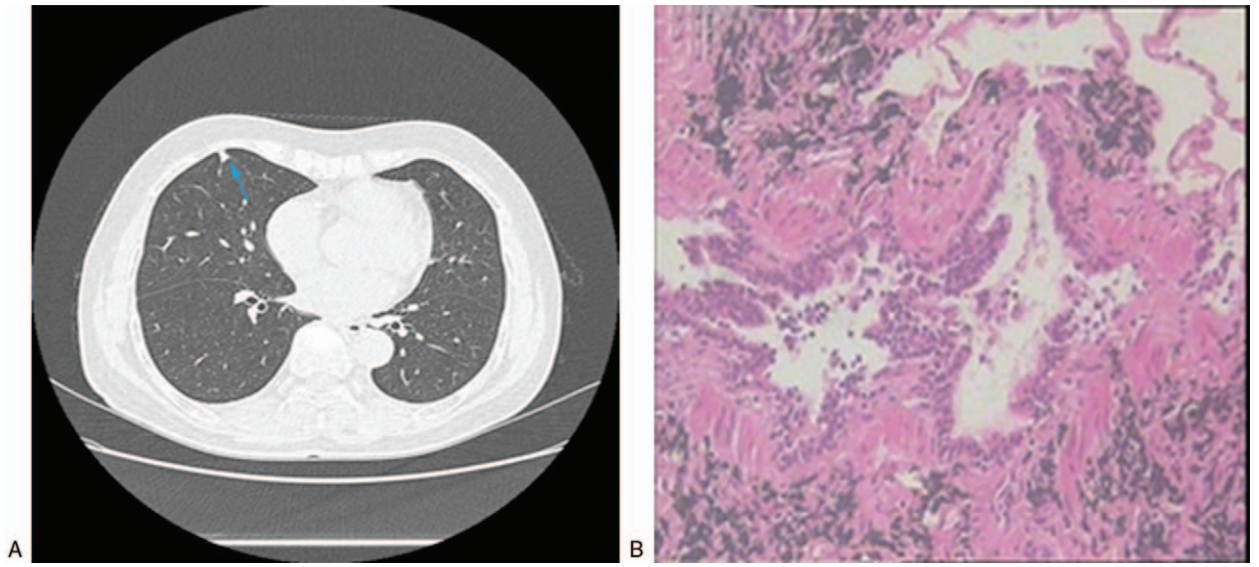

Figure 3. A 60-year-old nonsmoking woman with a peripheral solid nodule in the right middle lobe. (A) High-resolution computed tomography showed a 7-mm nodule with pleural adhesion and incisure surrounding (blue arrow). (B) The pathologic diagnosis of the resected specimen was fibrotic tissue.

Table 2

Univariable and multivariable logistic regression analyses of risk factors for malignant pulmonary nodules.

	Univariable			Multivariable		
	OR	95% CI	*P*	OR	95% CI	*P*
Age	0.98	0.953–1.009	.172			
Gender, male vs female	2.53	1.268–5.047	.008	2.613	0.964–7.078	.059
Smoking	0.34	0.136–0.850	.021	0.278	0.068–1.135	.075
Location, left vs right	1.055	0.562–1.981	.867			
Location			.251			
Lower	Ref					
Upper	1.029	0.508–2.084	.936			
Middle	0.471	0.168–1.320	.152			
Single vs multiple	0.473	0.217–1.028	.059			
Spiculation, yes vs no	1.000	0.398–2.510	1			
Cavitation sign, yes vs no	1.682	0.695–4.070	.249			
Calcification, yes vs no	0	0.000–∼	1			
Vascular penetration sign, yes vs no	3.155	1.551–6.417	.002	3.492	1.392–8.760	.008
Pleural adhesions, yes vs no	0.744	0.348–1.593	.447			
Incisure surrounding nodules, yes vs no	0.134	0.039–0.455	.001	0.179	0.038–0.841	.029
Nodule type			.005			.007
Pure ground glass/solid	Ref			Ref		
Mixed	3.051	1.395–6.669		4.270	1.484–12.285	
Long axis of pulmonary nodules	1.284	1.077–1.530	.005	0.594	0.163–2.167	.431
Short axis of pulmonary nodules	1.413	1.132–1.763	.002	2.662	0.584–12.125	.206
Ratio of short-axis to long-axis of the nodule	1.098	0.111–10.871	.936			
Nodule density	0.997	0.995–0.999	.001	0.995	0.993–0.998	.001

CI = confidence interval, OR = odds ratio.

This study proposes a pulmonary nodule prediction model that can estimate benign/malignant lung nodules with good sensitivity and specificity. Mixed ground-glass nodules, vascular penetration sign, density of lung nodules, and the absence of incisure signs are independently associated with malignant lung nodules. These results provide a better understanding of the judgment of benign vs malignant pulmonary nodules and could improve the rate of early lung cancer diagnosis.

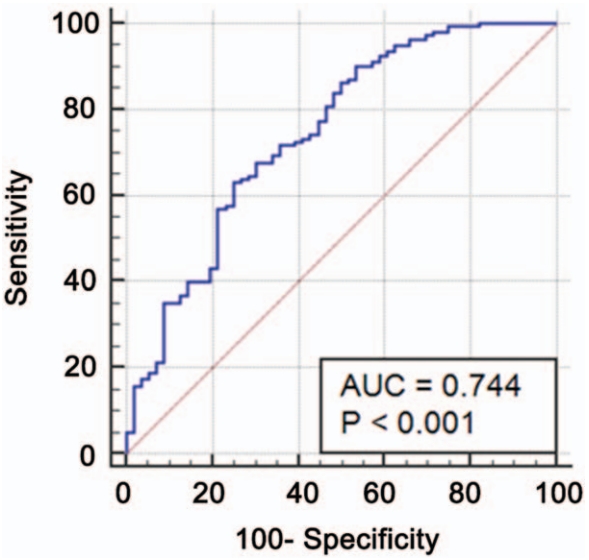

Figure 4. Receiver-operating characteristic curve of the prediction model for malignant nodules. Area under the curve (AUC) = 0.744 (96% confidence interval: 0.661–0.820).

Acknowledgment

The authors thank Hong-Wei Huang, Xiao-Rong Chen, and Yi-Lian Xia for their help with data collection.

Author contributions

Conceptualization: Weisong Chen.
Data curation: Dan Zhu.
Formal analysis: Dan Zhu, Jianfeng Luo.
Investigation: Haiwei Fu.
Methodology: Hui Chen.
Project administration: Weisong Chen.
Resources: Dan Zhu.
Supervision: Jianfeng Luo.
Validation: Hui Chen.
Writing – original draft: Weisong Chen.
Writing – review & editing: Weisong Chen, Haiwei Fu.

References

[1] Didkowska J, Wojciechowska U, Manczuk M, et al. Lung cancer epidemiology: contemporary and future challenges worldwide. Ann Transl Med 2016;4:150.
[2] Rolfo C, Passiglia F, Ostrowski M, et al. Improvement in lung cancer outcomes with targeted therapies: an update for family physicians. J Am Board Fam Med 2015;28:124–33.
[3] Siegel RL, Miller KD, Jemal A. Cancer statistics, 2018. CA Cancer J Clin 2018;68:7–30.
[4] Chen WQ, Li H, Sun KX, et al. Report of cancer incidence and mortality in China, 2014 [in Chinese]. Zhonghua Zhong Liu Za Zhi 2018;40:5–13.
[5] Qu RY, Zhou BS. Analysis of the distribution and trend of lung cancer mortality in China between 2004 and 2010 [in Chinese]. Chin J Health Stat 2014;31:932–5.
[6] Freedman ND, Leitzmann MF, Hollenbeck AR, et al. Cigarette smoking and subsequent risk of lung cancer in men and women: analysis of a prospective cohort study. Lancet Oncol 2008;9:649–56.

[7] Poinen-Rughooputh S, Rughooputh MS, Guo Y, et al. Occupational exposure to silica dust and risk of lung cancer: an updated meta-analysis of epidemiological studies. BMC Public Health 2016;16:1137.
[8] Kharazmi E, Fallah M, Sundquist K, et al. Familial risk of early and late onset cancer: nationwide prospective cohort study. BMJ 2012;345: e8076.
[9] Yang W, Qian F, Teng J, et al. Community-based lung cancer screening with low-dose CT in China: results of the baseline screening. Lung Cancer 2018;117:20–6.
[10] Liu S, Zhang M, Yang L, et al. Prevalence and patterns of tobacco smoking among Chinese adult men and women: findings of the 2010 national smoking survey. J Epidemiol Community Health 2017;71: 154–61.
[11] Li M, Liu X, Zhang L. The relationship of indoor coal use and environmental tobacco smoke exposure with lung cancer in China: a meta-analysis. J Cancer Res Therapeutics 2018;14:S7–13.
[12] Goldstraw P, Chansky K, Crowley J, et al. The IASLC Lung Cancer Staging Project: Proposals for Revision of the TNM Stage Groupings in the Forthcoming (Eighth) Edition of the TNM Classification for Lung Cancer. J Thorac Oncol 2016;11:39–51.
[13] Walters S, Maringe C, Coleman MP, et al. Lung cancer survival and stage at diagnosis in Australia, Canada, Denmark, Norway, Sweden and the UK: a population-based study, 2004-2007. Thorax 2013;68:551–64.
[14] Aberle DR, Adams AM, et al. National Lung Screening Trial Research TeamReduced lung-cancer mortality with low-dose computed tomographic screening. N Engl J Med 2011;365:395–409.
[15] Church TR, Black WC, et al. National Lung Screening Trial Research TeamResults of initial low-dose computed tomographic screening for lung cancer. N Engl J Med 2013;368:1980–91.
[16] Horeweg N, van Rosmalen J, Heuvelmans MA, et al. Lung cancer probability in patients with CT-detected pulmonary nodules: a prespecified analysis of data from the NELSON trial of low-dose CT screening. Lancet Oncol 2014;15:1332–41.
[17] MacMahon H, Naidich DP, Goo JM, et al. Guidelines for management of incidental pulmonary nodules detected on CT images: from the Fleischner Society 2017. Radiology 2017;284:228–43.
[18] Snoeckx A, Reyntiens P, Desbuquoit D, et al. Evaluation of the solitary pulmonary nodule: size matters, but do not ignore the power of morphology. Insights Imaging 2018;9:73–86.
[19] Parkar AP, Kandiah P. Differential diagnosis of cavitary lung lesions. J Belgian Soc Radiol 2016;100:100.
[20] Lin CH, Li TC, Tsai PP, et al. The relationships of the pulmonary arteries to lung lesions aid in differential diagnosis using computed tomography. Biomedicine 2015;5:11.
[21] Alberg AJ, Brock MV, Ford JG, et al. Epidemiology of lung cancer: diagnosis and management of lung cancer, 3rd ed: American College of Chest Physicians evidence-based clinical practice guidelines. Chest 2013;143:e1S–29S.
[22] Li F, Sone S, Abe H, et al. Low-dose computed tomography screening for lung cancer in a general population: characteristics of cancer in non-smokers versus smokers. Acad Radiol 2003;10:1013–20.
[23] Khuder SA. Effect of cigarette smoking on major histological types of lung cancer: a meta-analysis. Lung Cancer 2001;31:139–48.
[24] Kobayashi Y, Sakao Y, Deshpande GA, et al. The association between baseline clinical-radiological characteristics and growth of pulmonary nodules with ground-glass opacity. Lung Cancer 2014;83:61–6.
[25] Tamura M, Shimizu Y, Yamamoto T, et al. Predictive value of one-dimensional mean computed tomography value of ground-glass opacity on high-resolution images for the possibility of future change. J Thorac Oncol 2014;9:469–72.
[26] Guo H, Chang Z, Wu J, et al. Air pollution and lung cancer incidence in China: who are faced with a greater effect? Environ Int 2019; 132:105077.
[27] Cao Q, Rui G, Liang Y. Study on PM2.5 pollution and the mortality due to lung cancer in China based on geographic weighted regression model. BMC Public Health 2018;18:925.
[28] Seow WJ, Hu W, Vermeulen R, et al. Household air pollution and lung cancer in China: a review of studies in Xuanwei. Chin J Cancer 2014;33:471–5.
[29] Divisi D, Barone M, Bertolaccini L, et al. Standardized uptake value and radiological density attenuation as predictive and prognostic factors in patients with solitary pulmonary nodules: our experience on 1,592 patients. J Thorac Dis 2017;9:2551–9.
[30] Le V, Yang D, Zhu Y, et al. Quantitative CT analysis of pulmonary nodules for lung adenocarcinoma risk classification based on an exponential weighted grey scale angular density distribution feature. Comput Methods Programs Biomed 2018;160:141–51.
[31] Migliore M, Fornito M, Palazzolo M, et al. Ground glass opacities management in the lung cancer screening era. Ann Transl Med 2018;6:90.
[32] Larici AR, Farchione A, Franchi P, et al. Lung nodules: size still matters. Eur Respir Rev 2017;26:
[33] Truong MT, Ko JP, Rossi SE, et al. Update in the evaluation of the solitary pulmonary nodule. Radiographics 2014;34:1658–79.
[34] Patel VK, Naik SK, Naidich DP, et al. A practical algorithmic approach to the diagnosis and management of solitary pulmonary nodules: part 1: radiologic characteristics and imaging modalities. Chest 2013;143:825–39.
[35] Zhang M, Zhuo N, Guo Z, et al. Establishment of a mathematic model for predicting malignancy in solitary pulmonary nodules. J Thorac Dis 2015;7:1833–41.
[36] Lindell RM, Hartman TE, Swensen SJ, et al. Five-year lung cancer screening experience: CT appearance, growth rate, location, and histologic features of 61 lung cancers. Radiology 2007;242:555–62.
[37] Horeweg N, van der Aalst CM, Thunnissen E, et al. Characteristics of lung cancers detected by computer tomography screening in the randomized NELSON trial. Am J Respir Crit Care Med 2013;187:848–54.
[38] Yang L, Zhang Q, Bai L, et al. Assessment of the cancer risk factors of solitary pulmonary nodules. Oncotarget 2017;8:29318–27.
[39] McWilliams A, Tammemagi MC, Mayo JR, et al. Probability of cancer in pulmonary nodules detected on first screening CT. N Engl J Med 2013;369:910–9.